applied sciences

MDPI

Article

α-Glucosidase Inhibitors Based on Oleanolic Acid for the Treatment of Immunometabolic Disorders

Anastasiya V. Petrova [1], Denis A. Babkov [2,*], Elmira F. Khusnutdinova [1], Irina P. Baikova [1], Oxana B. Kazakova [1,*], Elena V. Sokolova [2] and Alexander A. Spasov [2]

[1] Ufa Institute of Chemistry, Ufa Federal Research Centre, Russian Academy of Science, 71 Pr., Oktyabrya Ufa 450054, Russia; ana.orgchem@gmail.com (A.V.P.); elmah@inbox.ru (E.F.K.); poljr@anrb.ru (I.P.B.)

[2] Scientific Center for Innovative Drugs, Volgograd State Medical University, 39, Novorossiyskaya St., Volgograd 400087, Russia; sokolova210795@gmail.com (E.V.S.); aspasov@mail.ru (A.A.S.)

* Correspondence: denis.a.babkov@gmail.com (D.A.B.); obf@anrb.ru (O.B.K.)

Abstract: Using oleanolic acid as a starting compound, a series of new oleanane-type triterpenic derivatives were synthesized via *O*-acylation (with nicotinic, isonicotinic, and methoxycinnamic acid acyl chlorides), *N*-amidation (with cyclic- or polyamines), the Mannich reaction (with secondary cyclic amines), and Claisen–Schmidt condensation (with aromatic aldehydes), and their potencies as treatments for immunometabolic disorders were investigated. The compounds were evaluated against α-glucosidase and PTP1B enzymes and LPS-stimulated murine macrophages. It was found that the target compounds are highly effective α-glucosidase inhibitors but lack activity against PTP1B. A leading compound, *N*-methylpiperazine methylated 2,3-indolo-oleanolic propargyl amide **15**, is also a micromolar inhibitor of NO synthesis in LPS-stimulated macrophages and suppresses oxidative bursts in neutrophils with similar efficiency. These results, in addition to its ability to stimulate glucose uptake in rat fibroblasts and improve maltose tolerance in rats, allow us to consider compound **15** a promising prototype drug for the treatment of immunometabolic defects in type 2 diabetes.

Keywords: triterpenoids; oleanolic acid; indole; Mannich reaction; type 2 diabetes; α-glucosidase inhibiting activity; PTP1B

Citation: Petrova, A.V.; Babkov, D.A.; Khusnutdinova, E.F.; Baikova, I.P.; Kazakova, O.B.; Sokolova, E.V.; Spasov, A.A. α-Glucosidase Inhibitors Based on Oleanolic Acid for the Treatment of Immunometabolic Disorders. *Appl. Sci.* **2023**, *13*, 9269. https://doi.org/10.3390/app13169269

Academic Editor: Emanuel Vamanu

Received: 3 July 2023
Revised: 29 July 2023
Accepted: 3 August 2023
Published: 15 August 2023

1. Introduction

Type 2 diabetes, marked by persistent hyperglycemia, is tied to obesity, insulin resistance, and systemic inflammation (metaflammation) that damages beta cells in the pancreas [1]. The disease contributes significantly to the prevalence of non-communicable diseases globally. Managing it often involves inhibiting α-glucosidase, an enzyme that helps convert complex carbohydrates into glucose. Existing pharmaceutical inhibitors, including acarbose and miglitol, help lower post-meal glucose levels but have drawbacks. They can be contraindicated for patients with gastrointestinal disorders and may not effectively control blood sugar levels. Thus, the pursuit of new compounds to act as α-glucosidase inhibitors for diseases like type 2 diabetes is critical [2]. They could potentially enhance glycemic control, decrease long-term complications, and improve overall disease management [3].

Currently, a large number of discoveries in the field of inhibitors are devoted to the synthesis of *N*-heterocyclic compounds. Benzimidazoles, thiadiazoles, thiazole, and triazoles are recommended as good inhibitors of α-glucosidase, acetylcholinesterase, and butyrylcholinesterase [4–7]. Among the various classes of compounds obtained from natural resources, triterpenoids also show potent antidiabetic activity, including α-glucosidase-inhibiting effects [8–11]. For example, oleanolic acid (OA) derivatives, such as oxime esters, showed inhibitory activities against α-glucosidase and α-amylase [12], a series of

benzylidene derivatives exhibited excellent to moderate inhibitory effects, and inhibition kinetics results showed that the leading analogs were reversible and mixed-type inhibitors of α-glucosidase and α-amylase [13,14]. OA indole derivatives with various electron-withdrawing groups possessed anti-α-glucosidase activities and demonstrated the capacity to form ligand-enzyme complexes with α-glucosidase enzymes [15]. However, in the field of metabolic disorders, researchers have not achieved such progress as with CDDO (an OA derivative), a potent anticancer agent which was evaluated in phase I clinical trials for the treatment of advanced solid tumors and lymphoma via the activation of Nrf2 in peripheral blood mononuclear cells and the inhibition of NF-κB and cyclin D1 in tumor biopsies [16]. All this proves that oleanolic acid is a promising scaffold for obtaining new pharmacological agents, and the search for new inhibitors based on it remains an urgent and priority task.

Keeping in mind the importance of these types of compounds, in this study, oleanolic acid derivatives containing nicotinic, isonicotinic, methoxycinnamic, succinic, polyamines, amides, arylidene, propargylaminoalkyl, and azepano fragments were synthesized, and their potencies as antidiabetic agents were investigated. It was found that the majority of the compounds exhibit significant α-glucosidase-inhibiting properties. The *N*-methylpiperazine methylated 2,3-indolo-oleanolic propargyl amide with the most potential, obtained via a one-pot Cu (I)-catalyzed Mannich reaction, was the most active compound acting as a noncompetitive inhibitor, with a *K*i (the dissociation constant of the enzyme-inhibitor complex) value estimated at 3.01 μM. The leading compound demonstrated that it can prevent inflammatory responses and the generation of ROS in immune cells and act synergistically with acarbose to ameliorate hyperglycemia. This exploration can provide alternative therapies while fostering a better understanding of immunometabolic disorders, thereby paving the path for targeted and potent treatments.

2. Materials and Methods

2.1. Chemistry

2.1.1. General

The spectra were recorded at the Center for the Collective Use 'Chemistry' at the Ufa Institute of Chemistry of the UFRC RAS and at the RCCU "Agidel" of the UFRC RAS. ^{1}H and ^{13}C NMR spectra were recorded using a "Bruker *Avance*-III" (Bruker, Billerica, MA, USA, 500 and 125.5 MHz, respectively, δ, ppm, Hz) in $CDCl_3$, internal standard tetramethylsilane. Mass spectra were obtained using an LCMS-2010 EV liquid chromatograph–mass spectrometer (Shimadzu, Kyoto, Japan). Melting points were detected on a microtable «Rapido PHMK05» (Nagema, Dresden, Germany). Optical rotations were measured via a Perkin-Elmer 241 MC polarimeter (PerkinElmer, Waltham, MA, USA) with a tube length of 1 dm. Thin-layer chromatography analyses were performed on Sorbfil plates (Sorbpolimer, Krasnodar, Russia), using the solvent system chloroform/ethyl acetate in a ratio of 40:1. Substances were detected via a 10% of sulfuric acid solution with subsequent heating at 100–120 °C for 2–3 min. All chemicals were of reagent grade (Sigma-Aldrich). Compounds **6, 7** [17], **8** [18], **9** [19], **10** [20], **11–13**, **15** and **16** [21]; **18** [22], **19** [23], **20**, **24,** and **27** [24]; **21**, **22**, and **25;** and **28** [25], **29,** and **30** [22] were prepared as described previously. All spectral data are provided in the Supplementary Materials file.

2.1.2. General Procedure for the Synthesis of Compounds **4** and **5**

To a solution of compound **2** (1 mmol; 0.44 g) in dry pyridine (15 mL), 3-(3-methoxyphenyl) acryloyl chloride (2 mmol; 0.39 g) or nicotinoyl chloride (2 mmol; 0.28 g) and DMAP (cat.) was added. The reaction mixture was refluxed for 4 h, poured into H_2O/H^+, filtered, washed with water until neutral, and dried. The residue was purified via Al_2O_3 column chromatography (eluent petroleum ether-ethyl acetate 20:1→5:1).

3,28-Di-O-[3-(3-methoxyphenyl)acrylate]-olean-12(13)-en **4**

Beige solid; mp: 114 °C; yield 78%; $[\alpha]_D^{20}$ +17° (*c* 0.1, $CHCl_3$). ^{1}H NMR (500 MHz, $CDCl_3$) δ 7.64 (m, 2H, H3″, H8″), 7.62 (m, 2H, H3′, H8′), 7.48 (d, *J* = 8.7 Hz, 2H, H9′, H9″), 6.92 (d, *J* = 1.5 Hz, 2H, H5′, H5″), 6.86 (d, *J* = 1.7 Hz, 2H, H7′, H7″), 6.33 (d, *J* = 2.7 Hz, 1H, H2″), 6.29 (d, *J* = 2.5 Hz, 1H, H2′), 5.23 (s, 1H, H12), 4.64 (dd, *J* = 9.2 Hz, 1H, H3), 4.17 (d, *J* = 11.0 Hz, 1H, H28), 3.83 (2s, 6H), 3.80 (m, 1H, H28), 2.16–1.00 (m, 23H, CH, CH_2), 1.18, 0.99, 0.98, 0.94, 0.91, 0.90, 0.88 (7s, 21H, $7CH_3$). $^{13C\ NMR\ (125.5\ MHz,\ CDCl_3)}$ δ 167.50 (C1′), 167.20 (C1″), 161.32 (C6″), 161.27 (C6′), 144.14, 143.96, 143.67 (C13), 131.97, 129.71, 129.68, 127.30, 127.25, 122.86 (C12), 116.35, 115.87, 114.30, 113.47, 113.40, 80.74 (C3), 70.68 (C28), 55.37 (OCH_3), 55.32 (C5), 47.55 (C18), 46.27 (C19), 42.60, 41.69, 39.83, 38.34, 37.98, 36.86 (C10), 36.08, 34.05, 33.18, 32.50, 31.55, 30.95 (C20), 28.10, 25.99, 25.65, 23.71, 23.60, 22.37, 18.25, 16.89, 16.82, 16.74, 15.60. MS (APCI) *m/z* 763.6 $[M+H]^+$ (calcd for $C_{50}H_{66}O_6$, 763.07).

3,28-Di-O-[isonicotinate]-olean-12(13)-en **5**

Beige solid; mp: 123°C; yield 72%; $[\alpha]_D^{20}$ +5° (*c* 0.1, $CHCl_3$). ^{1}H NMR (500 MHz, $CDCl_3$) δ 8.80–8.73 (m, 4H, H4″, H6″, H4′, H6′), 7.85–7.80 (m, 4H, H3″, H7″, H3′, H7′), 5.25 (s, 1H, H12), 4.79–4.72 (m, 1H, H3), 4.33 (d, *J* = 11.0 Hz, 1H, H28), 3.97 (d, *J* = 11.1 Hz, 1H, H28), 1.02–2.18 (m, 23H, CH, CH_2), 1.19, 1.01, 0.99, 0.93, 0.91 (7s, 21H, $7CH_3$). ^{13}C NMR (125.5 MHz, $CDCl_3$) δ 165.06 (C1″), 164.75 (C1′), 150.67 (C6″, C4″), 150.56 (C6′), 150.51 (C4′), 143.37 (C13), 138.14 (C2′), 137.76 (C2′), 123.07 (C12), 122.86 (C3″, C7″, C3′, C7′), 82.72 (C3), 71.98 (C28), 55.29 (C5), 47.51 (C18), 46.15 (C19), 42.59, 41.69, 40.13, 39.83, 38.25, 38.10, 37.45, 36.85 (C10), 36.24, 34.15, 33.94, 33.13, 32.43, 31.62, 30.91 (C20), 28.20, 26.20, 26.02, 25.62, 23.57, 23.52, 22.45, 21.50, 18.20, 16.94, 16.73, 15.57. MS (APCI) *m/z* 653.5 $[M+H]^+$ (calcd for $C_{42}H_{56}N_2O_4$, 652.92).

2.1.3. Synthesis of Compound **17**

N-Methylpiperazine (1.6 mmol; 0.16 mL), paraformaldehyde (0.3 g), NaOAc (5 mmol; 0.41 g), and CuI (0.05 mmol; 9.5 mg) were added to a solution of compound **11** (1 mmol; 0.56 g) in dry dioxane (10 mL). The reaction mixture was stirred under argon for 10 h at 60 °C. After the reaction, the mixture was diluted with water and extracted with $CHCl_3$ (3 × 20 mL). The combined organic layer was washed with water (3 × 50 mL), dried over $CaCl_2$ and evaporated under reduced pressure. The residue was purified by SiO_2 column chromatography (eluent $CHCl_3$–MeOH 100:0→90:10), obtaining compound **17.**

[3,2b]Indolo-N-(4-(piperazin-1-yl)but-2-yn-1-yl)-olean-12(13)-en-28-amide **17**

Yellow solid; mp: 139°C; yield 81%; $[\alpha]_D^{20}$ −21° (*c* 0.1, $CHCl_3$). ^{1}H NMR (500 MHz, $CDCl_3$) δ 7.45–7.00 (m, 4H), 6.12 (br. s, NH), 5.50 (s, 1H, H12), 3.90 and 4.10 (d, 2H, *J* = 17.2 Hz, $NHCH_2$), 3.30 (d, *J* = 9.1 Hz, NCH_2), 2.80−2.50 (m, 8H, $4CH_2$), 2.30−1.30 (m, 23H, CH and CH_2), 1.32, 1.30, 1.22, 1.20, 0.90, 0.89, 0.81 (7s, 21H, $7CH_3$). ^{13}C NMR (125.5 MHz, $CDCl_3$) δ 178.03 (CONH), 144.62 (C13), 140.90, 136.16, 128.10, 123.30 (C12), 120.92, 118.81, 117.85, 110.47, 106.50, 81.10 (C≡C), 79.11 (C≡C), 53.07 (2C), 51.32 (2C), 46.91, 46.66, 46.39, 46.24, 42.20, 40.94, 39.50, 38.01, 37.45, 36.82, 34.11, 34.01, 33.01, 32.26, 31.78, 30.97, 30.76, 29.63, 27.32, 25.60, 23.93, 23.62, 23.31, 19.29, 16.63, 15.67. MS (APCI) *m/z* 663.5 $[M+H]^+$ (calcd for $C_{44}H_{62}N_4O$, 663.01).

2.1.4. General Procedure for the Synthesis of Compounds **14** and **26**

To a solution of compound 3 (1 mmol; 0.53 g), oleanonic acid (1 mmol; 0.45 g), or **21** (1 mmol; 0.54 g) in dry CH_2Cl_2 (15 mL), $(COCl)_2$ (0.08 mL, 1 mmol), and Et_3N (2 drops) were added. The reaction mixture was stirred at room temperature for 2 h, then CH_2Cl_2 was evaporated to give an intermediate acyl chloride. This residue was dissolved in CH_2Cl_2 (5 mL) and a CH_2Cl_2 solution of piperazine (1.3 mmol; 0.11 g), 2-aminopyridine (1.3 mmol; 0.12 g) or ammonia solution (1.3 mmol; 0.02 mL), and Et_3N (1 mmol; 0.14 mL) was added in each reaction. The reaction mixture was refluxed for 2 h, the organic layer was diluted with cold water (20 mL) and separated. The aqueous layer was extracted

with CH_2Cl_2 (2 × 15 mL), the combined extracts were washed with 5% HCl (3 × 15 mL), H_2O (2 × 15 mL), dried over $CaCl_2$, and the solvent was evaporated in a water jet vacuum. Purification of the crude product was performed using column chromatography on Al_2O_3 by elution with a mixture of petroleum ether–chloroform (1:0 → 1:1).

[3,2b]Indolo-N-piperazin-olean-12(13)-en-28-amide **14**

Yellow solid; mp: 117 °C; yield 85%; $[\alpha]_D^{20}$ +4° (*c* 0.1, $CHCl_3$). ^{1}H NMR (500 MHz, $CDCl_3$) δ 7.45–7.00 (m, 4H), 5.38 (s, 1H, H12), 3.15–2.70 (m, 8H, $4CH_2$), 3.10−1.20 (m, 22H, CH and CH_2), 1.30, 1.21, 1.19, 0.95, 0.93, 0.91, 0.81 (7s, 21H, $7CH_3$). ^{13}C NMR (125.5 MHz, $CDCl_3$) δ 175.34 (C28), 144.17 (C13), 140.91 (C3), 136.12 (C6′), 128.22 (C1′), 122.09 (C12), 120.89 (C4′), 118.82 (C3′), 117.98 (C2′), 110.36 (C5′), 106.81 (C2), 53.27 (2C), 51.63 (2C), 47.59, 46.47, 46.32, 44.60, 43.70, 42.05, 39.26, 38.15, 36.73, 34.01, 33.04, 32.36, 31.01, 30.41, 29.99, 27.99, 25.82, 24.03, 23.44, 23.32, 22.83, 19.31, 16.74, 16.68, 15.59. MS (APCI) *m/z* 596.5 $[M+ H]^+$ (calcd for $C_{40}H_{57}N_3O$, 595.92).

2-[(E)-pyridine-4-ylmethylene]-3-oxo-olean-12(13)-en-28-carboxamide **26**

White solid; mp: 166 °C; yield 72%; $[\alpha]_D^{20}$ +49° (*c* 0.1, $CHCl_3$). ^{1}H NMR (500 MHz, $CDCl_3$) δ 8.71–8.65 (d, *J* = 6 Hz, 2H), 7.40–7.30 (d, *J* = 6.2 Hz, 2H), 6.95 (s, 1H), 5.85 (br.s, NH), 5.40 (d, *J* = 3.4 Hz, 1H, H12), 2.95–1.25 (m, 22H, CH, CH_2), 1.24, 1.18, 1.15, 0.90, 0.95, 0.88, 0.87 (7s, 21H, $7CH_3$). ^{13}C NMR (125.5 MHz, $CDCl_3$) δ 207.09 (C3), 181.01 (C28), 147.92, 145.54, 145.04 (C13), 142.22, 139.08, 133.21, 126.21, 124.69, 122.19 (C12), 53.00, 46.62, 46.49, 45.42, 44.03, 42.69, 42.37, 39.36, 39.13, 36.35, 34.07, 32.97, 32.51, 31.56, 30.73, 29.50, 27.28, 25.72, 25.49, 23.50, 22.68, 20.24, 19.05, 16.59, 15.39. MS (APCI) *m/z* 543.5 $[M+ H]^+$ (calcd for $C_{36}H_{50}N_2O_2$, 542.81).

2.1.5. Synthesis of Compound **23**

4-Pyridinecarboxyaldehyde (1.3 mmol; 0.12 mL) and 40% KOH in ethanol (2.5 mL) were added to a solution of compound **19** (1 mmol; 0.53 g) in ethanol (5 mL) under stirring and cooling (from −5 to 10 °C). The mixture was stirred for 24 h at room temperature, pH was adjusted to neutral values with 5% HCl solution, and the mixture was poured into cold water (50 mL). The residue was filtered, washed with water and dried, then purified by column chromatography on Al_2O_3 using petroleum ether-CHCl3 (1:1 to 1:3) as eluent.

N-(pyridin-2-yl)-2-[(E)-pyridine-3-ylmethylene]-3-oxo-olean-12(13)-en-28 carboxamide **23**

Beige solid; mp: 154–156°C; yield 71%; $[\alpha]_D^{20}$ +23° (*c* 0.1, $CHCl_3$). ^{1}H NMR (500 MHz, $CDCl_3$) δ 8.63 (d, *J* = 4.8 Hz, 2H, H4″–H6″), 8.49 (d, *J* = 4.8 Hz, 2H, H3″- H7″), 8.30 (s, 1H, NH), 8.20–8.25 (m, 2H, H3′–H6′), 7.65 (m, 1H, H4′), 7.25 (s, 1H, H1″), 6.99 (m, 1H, H5′), 5.58 (s, *J* = 3.21 Hz, 1H, H12), 2.93 (d, *J* = 15.5 Hz, 1H, H1), 2.82 (d, *J* = 10.4 Hz, 1H, H18), 2.28 (d, *J* = 15.5 Hz, 1H, H1), 1.00–2.30 (m, 18H, CH, CH_2), 1.23, 1.12, 0.93, 0.92, 0.82, 0.91, 0.69 (7s, 21H, $7CH_3$). ^{13}C NMR (125.5 MHz, $CDCl_3$) δ 207.41 (C3), 176.75 (C28), 151.43 (C1′), 149.82 (C4″, C6″), 148.69 (C2), 147.49 (C3′), 144.15 (C13), 143.50 (C2″), 138.48 (C5′), 137.96 (C1″), 124.11 (C3″, C7″), 122.89 (C12), 119.61 (C4′), 113.97 (C6′), 52.98 (C5), 47.40, 46.53, 45.38, 45.31, 43.96, 42.20 (C4), 42.10, 39.27, 36.31, 34.09, 32.99, 32.52, 31.48, 30.74, 29.48, 27.39, 25.73, 24.03, 23.78, 23.57, 22.02, 20.19, 16.09, 15.36. MS (APCI) *m/z* 620.5 $[M+H]^+$ (calcd for $C_{41}H_{53}N_3O_2$, 619.89).

2.2. Biological Evaluation

Biological Assays

The experimental procedures for α-Glucosidase assay, PTP1B inhibition assay, cellular assay, animal assay, and statistical analysis are included in Supplementary Materials Data: S2 Biological evaluation.

3. Results and Discussion

3.1. Chemistry

Our previous studies confirm that compounds containing such groups as isonicotinic, methoxycinnamic, succinic, polyamine, arylidene, amide, propargylaminoalkyl, and azepane display cytotoxic and antimicrobial activity [25,26]. Also, we have shown that among the different types of triterpenoids [27–29], 2,3-indolo-betulinic acid glycine and *L*-phenylalanine amides were discovered as lead compounds with IC_{50} values of 0.04 and 0.05 μM, being 3784- and 4730-fold more active than acarbose [30]. Triterpene type indoles were highlighted as excellent pharmacophore platforms for the development of new anti-diabetes drugs [31]. We have shown that lupane-type C2-furfurylidene, *m*-iodobenzylidene, and 3-pyridinylidene derivatives exhibited significantly better activity (up to 700 times higher) than acarbose [32], as well as the chalcone derivatives of platanic acid (20-oxo-lupanes) with furfurylidene and trifluoromethylbenzylidene fragments [33].

Thus, to study the inhibitory activity of α-glucosidase, a series of oleanolic acid derivatives with these pharmacophore groups was obtained.

Triterpenic platforms such as oleanolic acid **1**, erythrodiol (ED) **2**, 2,3-indolo- and C2-benzylidene derivatives of 3-oxo-OA were successfully used for the synthesis of the desired compounds **4–18** and **19–28** (Schemes 1–3). Scheme 1 outlines the synthesis of compounds **4–10** by *O*-acylation and *N*-amidation of hydroxy and carboxy groups at C3 and C28 positions of OA **1** and ED **2**. The reaction of nicotinic, isonicotinic, and methoxycinnamic acid acyl chlorides or succinic anhydride with **1** or **2** led to mono- and bis-esters **4–8**. Amides **9** and **10** were obtained from 3-acetoxyoleanolic acid by the reaction of **1** with spermidine or diethyltriamine by the acyl chloride method in the presence of Et_3N.

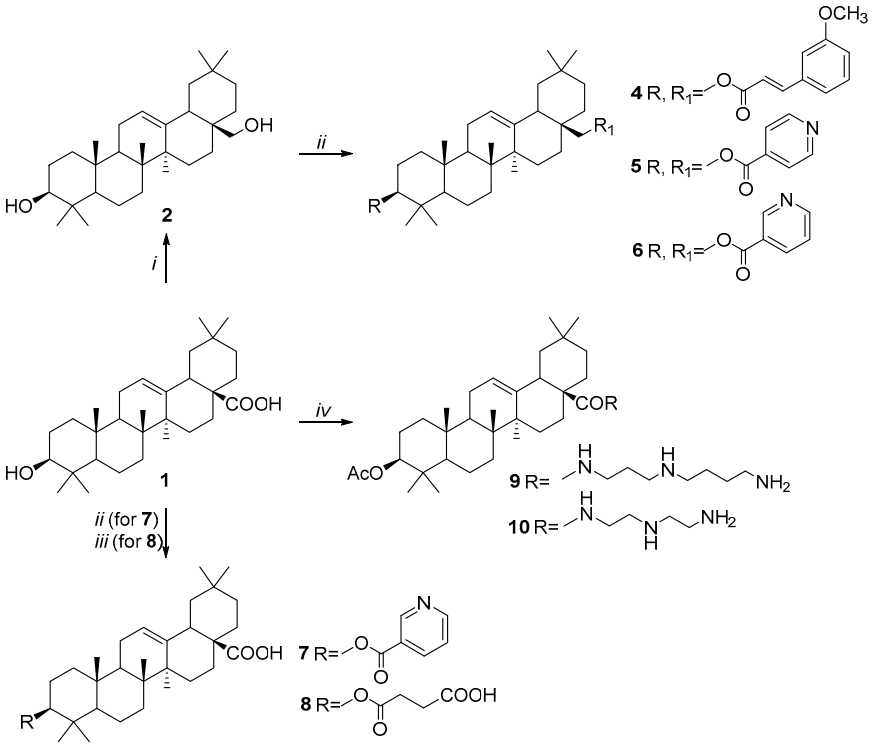

Scheme 1. Synthesis of OA and ED derivatives **4–10**. Reagents and conditions: (i) $LiAlH_4$, THF, reflux; (ii) 3-(3-methoxyphenyl)acryloyl or nicotinoyl chlorides, DMAP, Py, reflux; (iii) succinic anhydride, Py, reflux; (iv) 1. Ac_2O, Py, reflux; 2. $(COCl)_2$, CH_2Cl_2, 25 °C; 3. spermidine or diethyltriamine, Et_3N, CH_2Cl_2, 25 °C.

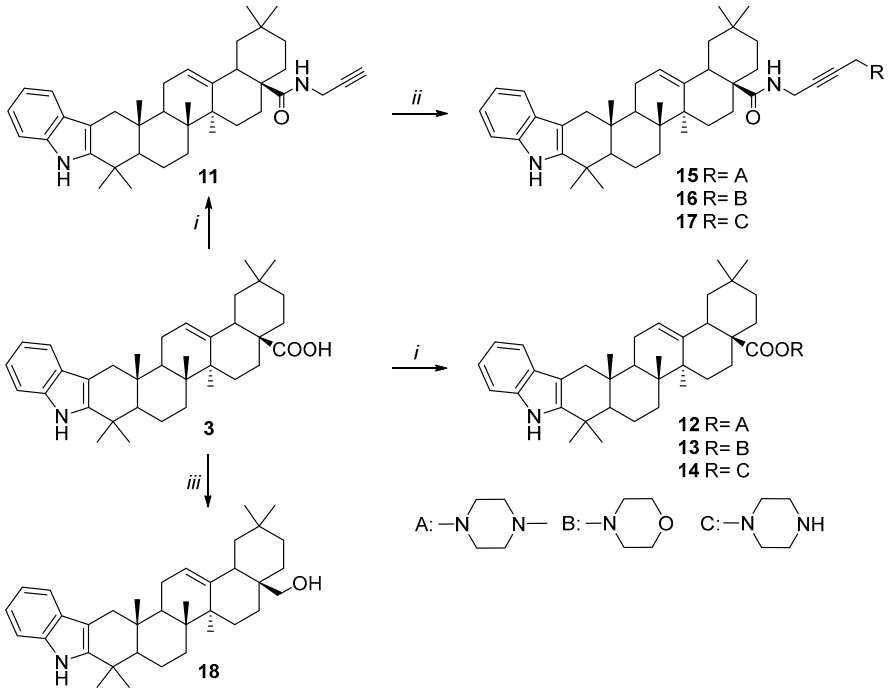

Scheme 2. Synthesis of 2,3-indolo-oleanolic acid derivatives **12–18**. Reagents and conditions: (i) 1. $(COCl)_2$, CH_2Cl_2, 25 °C; 2. corresponding amine, Et_3N, CH_2Cl_2; 25 °C; (ii) corresponding amine, PFA, NaOAc, CuI, 1,4-dioxane, 60 °C; (iii) $LiAlH_4$, THF, reflux.

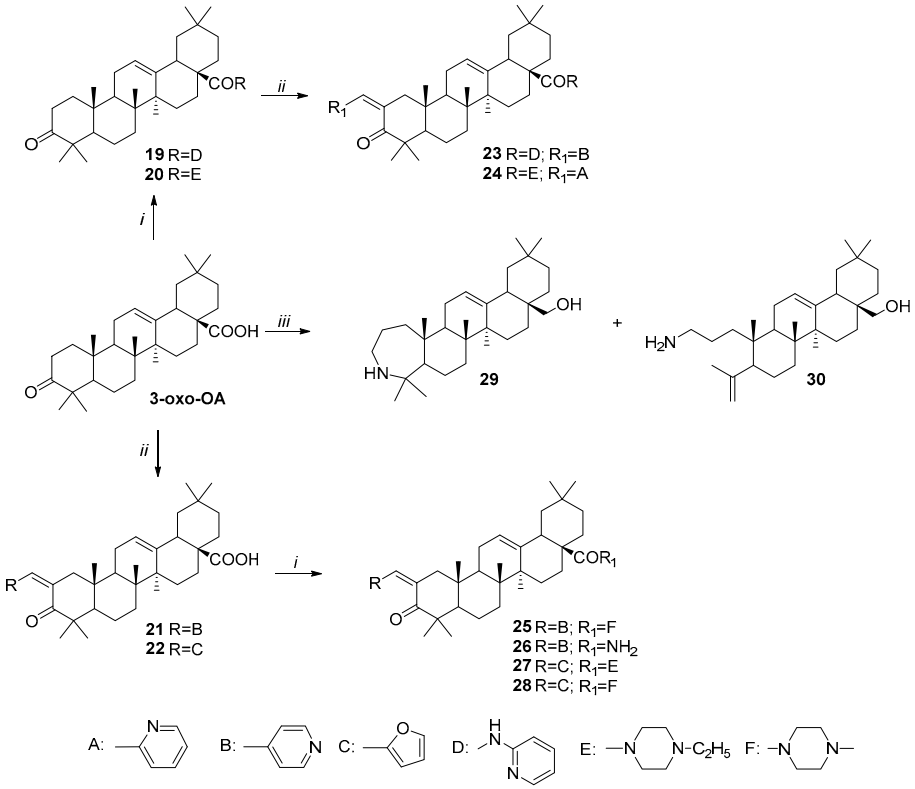

Scheme 3. Synthesis of A-ring modified OA derivatives **19–30**. Reagents and conditions: (i) 1. $(COCl)_2$, CH_2Cl_2, 25 °C; 2. Corresponding amine, Et_3N, CH_2Cl_2, 25 °C; (ii) corresponding aldehyde, 40% KOH in EtOH, EtOH; (iii) 1. $NH_2OH{\cdot}HCl$, NaOAc, EtOH, reflux; 2. $SOCl_2$, 1,4-dioxane; 3. $LiAlH_4$ THF, reflux.

Compounds **12–18** were prepared from 2,3-indolo-oleanolic acid **3** [15] (Scheme 2). First, the coupling of **3** with secondary amines by the acyl chloride method led to amides **12–14**. The Mannich reaction of alkynylamide **11** with amines in the presence of a catalytic amount of copper iodide and sodium acetate produced propargylaminoalkyl derivatives **15–17**.

Scheme 3 describes the Claisen–Schmidt condensation of 3-oxo-OA amide **19** and **20** derivatives with 2- or 4-pyridinecarboxaldehyde or furfural to afford C2-substituted compounds **23–28**. Additionally, two other A-ring modified azepano- **29** and seco- **30** derivatives were synthesized [22].

3.2. Biological Evaluation

3.2.1. Enzymatic Screening

Based on our previous results [30], the synthesized compounds were evaluated as α-glucosidase inhibitors. Screening in 100 μM concentration was performed, followed by IC_{50} evaluation for active compounds. As Table 1 shows, the majority of oleanolic acid derivatives proved to be effective α-glucosidase inhibitors, significantly exceeding the activity of acarbose.

Table 1. Biological activity of compounds **4–30**.

Cmpd	Glucosidase IC_{50} ± SD, μM	% NO (10 μM)	% MTT Viability (10 μM)	MTT CC_{50} (μM)	NO IC_{50} (μM)
4	2.4 ± 0.47	insoluble	insoluble		
5	4.56 ± 1.1	insoluble	insoluble		
6	752.6 ± 536.5	insoluble	insoluble		
7	>600	66.83	43.79		
8	6.5 ± 4.4	−51.7	4.74		
9	4.5 ± 0.9	105.42	116.07		
10	>600	−30.35	1.88		
11	139.1 ± 73.82	34.22	103.18	>100	>100
12	4.71 ± 1.17	98.19	90.61		
13	170.2 ± 36.04	89.13	100.77		
14	38.3 ± 6.9	51.97	16.56		
15	3.01 ± 0.53	26.11	18.24	4.66	4.83
16	13.91 ± 3.08	insoluble	insoluble		
17	223.5 ± 44.19	insoluble	insoluble		
18	12.37 ± 3.34	33.37	72.59		>100
19	14.2 ± 6.71	insoluble	insoluble		
20	18.88 ± 7.35	59.67	140.65		39.11
21	5.56 ± 1.88	75.26	94.15		
22	inactive	42.56	111.77		>100
23	6.6 ± 1.12	−4.33	6.17		
24	inactive	7.69	194.19	>100	7.89
25	79.35 ± 14.04	54.7	98.83		38.17
26	38.84 ± 6.63	insoluble	insoluble		
27	>600	−6.13	124.59	35.2	10.71
28	inactive	77.79	82.68		
29	inactive	−133.47	22.47		
30	20.5 ± 1	−66.87	2.38		
Acarbose	436	—	—	—	—
Dexamethasone	—	2.01	98.77	>100	0.003

The structure–activity relationship of compounds **4–30** was analyzed according to the experimental data in Table 1. One can see that the enzyme inhibition was increased when the 3,28-dihydroxy-groups of erythrodiol were esterified with *m*-methoxy-cinnamic acid (compound **4**) and isonicotinic acid (compound **5**). Compounds **4** and **5** exhibited much better potent inhibitory activity with IC_{50} values of 2.40 ± 0.47 μM, 4.56 ± 1.1 μM, respectively, which were about 96- to 182-fold higher than that of acarbose (IC_{50} 436 μM). Compound **6** with 3,28-bisnicotinic moieties was not active (IC_{50} 752.6 μM). The replacement of C28

to a free carboxy group in the case of compound **7** was not successful (IC_{50} >600 μM). OA succinate **8** is more active than **7** with IC_{50} value 6.50 ± 0.47 μM being 98-fold more efficient than the acarbose. 3β-Acetoxy-OA spermidine amide **9** exhibited significantly better activity (IC_{50} 4.50 ± 0.9 μM) than another long-chain polyamine amide **10** (IC_{50} > 600 μM).

Modification of 2,3-indolo-OA propargyl amide **11** (IC_{50} 139.1 ± 73.82 μM) to Mannich bases with *N*-methylpiperazine- **15** and morpholine- **16** moieties led to an increase in activity with IC_{50} values of 3.01 ± 0.53 μM and 13.91 ± 3.08 μM, respectively, that were about 31- to 145-fold higher than that of acarbose. At the same time, compound **17** with piperazine fragment showed only a weak activity. When the heterocycles, such as *N*-methylpiperazine and morpholine, were conjugated directly with an oleanane core via amide function at C28 (compounds **12** and **13**), the inhibitory activity against α-glucosidase decreased. Meanwhile, piperazine amide **14** exhibited higher activity (IC_{50} 38.3 ± 6.9 μM) than the propargyl containing analogue **17**. The derivatives of erythrodiol with indole **18** and seco-amine **30** fragments showed potent activity with IC_{50} values of 12.37 ± 3.34 μM and 20.5 ± 1 μM, respectively, whereas compound **29** with A-azepano-cycle was inactive.

Among the series of C2-derivatives **21-28** obtained using Claisen–Schmidt condensation, 4-pyridinylideno-OA **21** demonstrated an activity with an IC_{50} value of 5.56 ± 1.88 μM, being 78-fold more active than acarbose. The enzyme inhibition activity decreased when the carboxyl group of the compound **21** was amidated using pyridine-2-amine up to **23** (IC_{50} 6.6 ± 1.12 μM), *N*-methyl-piperazine up to **25** (IC_{50} 79.35 ± 14.04 μM), or in the case of carboxamide derivative **26** (IC_{50} 38.84 ± 6.63 μM). The introduction of the furfurylidene fragment (compound **22)**, as well as the modification of the carboxyl group to *N*-ethyl- **27** or *N*-methyl-piperazine amide **28**, led to a negative effect on inhibitory activity. Pyridine **19** or *N*-ethyl-piperazine **20** amides exhibited high activity with an IC_{50} of 14.2 ± 6.71 μM and 18.88 ± 7.35 μM. Modification of **20** by introducing 2-pyridinylidene- **24** or furfurylidene **27** fragments led to the loss of activity, while the presence of isomeric 4-pyridinylideno fragments increased the activity of **23** (IC_{50} 6.6 ± 1.12 μM) compared to **19** almost twice.

Several studies identified triterpenoid inhibitors of PTP1B, a valuable antidiabetic target [34–36]. We have also screened compounds against this enzyme, but no activity was observed up to 100 μM (). This may be attributed to the lack of a 3-hydroxy group, which appears to be a requisite for PTP1B inhibition [37].

3.2.2. Influence on LPS-Stimulated Macrophages

Considering the pivotal role of immunometabolic disorders in type 2 diabetes, target compounds were also profiled using a phenotypic screening approach [38]. Primary peritoneal murine macrophages were stimulated with LPS to induce a pro-inflammatory state. Target compounds were tested for the suppression of LPS-induced nitric oxide (NO) synthesis at a screening concentration of 10 μM. According to the MTT test, seven compounds (compounds **11, 18, 20, 22, 24, 25,** and **27**) inhibit the formation of NO by LPS-activated peritoneal macrophages in mice. Of these, compound **24** with an IC_{50} value of 7.8 μM was the most active, but this compound has no activity against a-glucosidase. Compound **20** is also non-cytotoxic, suppresses the synthesis of NO with an IC_{50} 39.11 μM, and inhibits a-glucosidase with an IC_{50} of 18.88 μM.

Compound **15**, the most potent glucosidase inhibitor, also actively suppressed NO synthesis (IC_{50} 4.8 μM), but according to the MTT test, it also reduced cell metabolic activity. Final conclusions about cytotoxicity can be made after the involvement of additional research methods. The MTT test can both overestimate and underestimate the actual cell viability. In particular, such artifacts have been described for triterpene acids [39–41]. In general, 2,3-indolo-oleanolic acid derivatives appear to be more active than A-ring modified oleanolic acid derivatives. The anti-inflammatory activity was improved upon the introduction of the *N*-alkyl-piperazine moiety at C28 carboxyl, as exemplified by compounds **15** and **24**.

We observed a lack of correlation between α-glucosidase and NO inhibition. Similar results were reported for betulinic acid derivatives [42]. Compound **15** appeared to be

dual active and the most potent one, hence, it was nominated as a lead for further studies. There are a considerable number of studies on the role of intracellular glucosidase enzymes in pancreatic islet metabolism and macrophage immune response [43,44], also see [45], however the precise mechanistic basis of intracellular endoplasmic reticulum glucosidase involvement in NO synthesis remains to be elucidated. Also, multiple other protein targets can be engaged by triterpenoids, and the factor of the various cellular permeabilities of the studied compounds cannot be ruled out.

3.2.3. Mechanism of α-Glucosidase Inhibition by Compound **15**

The mechanism of the inhibition of α-1,4-glucosidase of *S. cerevisiae* by lead compound **15** was elucidated using a kinetic experiment. Results show that **15** behaves as an uncompetitive (mixed-type) inhibitor. The linear correlation of the reaction slope with the concentration of the inhibitor suggests the presence of one allosteric binding site. The inhibition constant K_i was estimated at 3.011 μM (Figure 1).

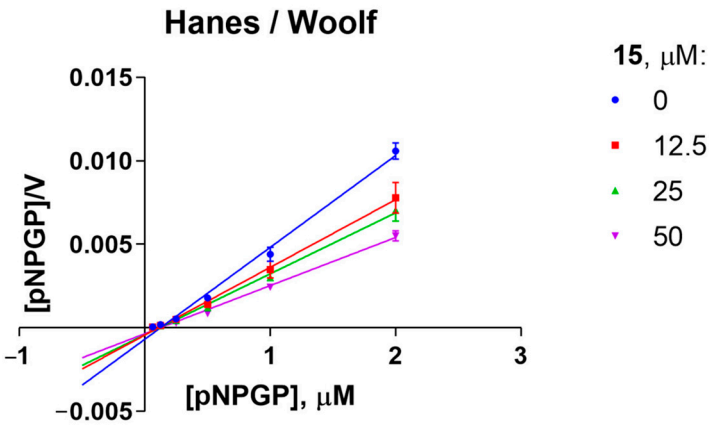

Figure 1. Hanes–Woolf plot of kinetic experiment on the inhibition of *S. cerevisiae* α-glucosidase by compound **15**. Analysis conditions: [E] 0.25 μM, [S] 1000.0 μM, K_m 0.1166 μM.

The studied compounds are inactive against rat intestinal maltase (IC_{50} for acarbose is 7 μM), i.e., they will not affect the absorption of carbohydrates from the intestine.

3.2.4. Cytotoxic Evaluation of Compound 15 towards Macrophages

To determine whether MTT-based cytotoxicity data for compound **15** is reliable, additional experiments were performed with primary peritoneal macrophages. Neutral red (NR) is a cationic dye whose uptake is known to reflect ATP-dependent lysosomal function. The test with neutral red revealed a similar concentration response as was observed in the NO and MTT assays (Figure 2). MTT and neutral red uptake assays both show viability with CC_{50} values around 5 μM.

To confirm these findings, we have also assessed the morphological alterations of macrophages treated with **15** or dexamethasone, since this is considered the most reliable method for evaluating cytotoxicity [46]. The final concentration of compound **15** was set at 10 μM, which resulted in a complete loss of apparent viability according to MTT and neutral red uptake, and also a complete suppression of NO synthesis. In the LPS-treated control sample, the cells acquire an elongated fusiform stellate shape, the cells are spread out and are tightly attached to the culture plate (Figure 3). Surprisingly, both compound **15** and dexamethasone did not change the rounded shape of the cells to stellate under LPS stimulation, which may reflect a lack of M1-polarization and explain the suppression of NO synthesis. However, there are cells with nuclei on the periphery, loss of cytoplasm, and vacuolization of the membrane, this may indicate the presence of the first phase of apoptosis. It should be noted that similar features are evident in some of the intact and dexamethasone-treated cells as well. Cell morphology in the presence of 10 μM **15** remains

normal and corresponds to the morphological features of intact cells. Final conclusions about cytotoxicity can be made after the involvement of additional research methods.

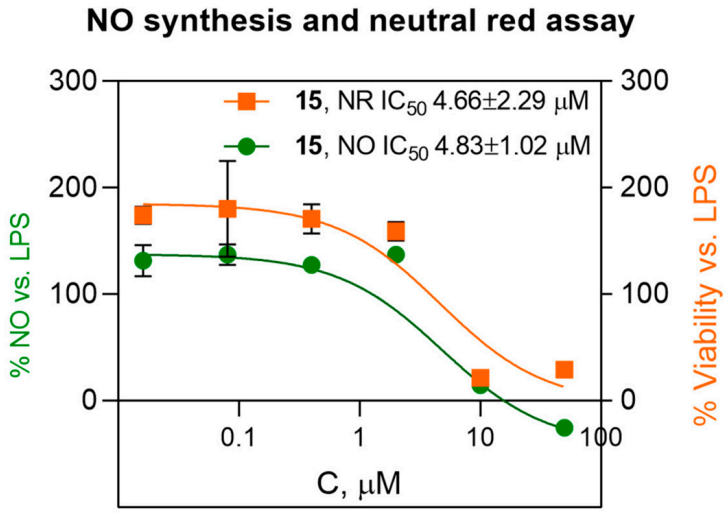

Figure 2. Compound **15** inhibit NO synthesis and neutral red (NR) viability of LPS-stimulated peritioneal macrophages. Data are shown as mean ± SD (n = 3).

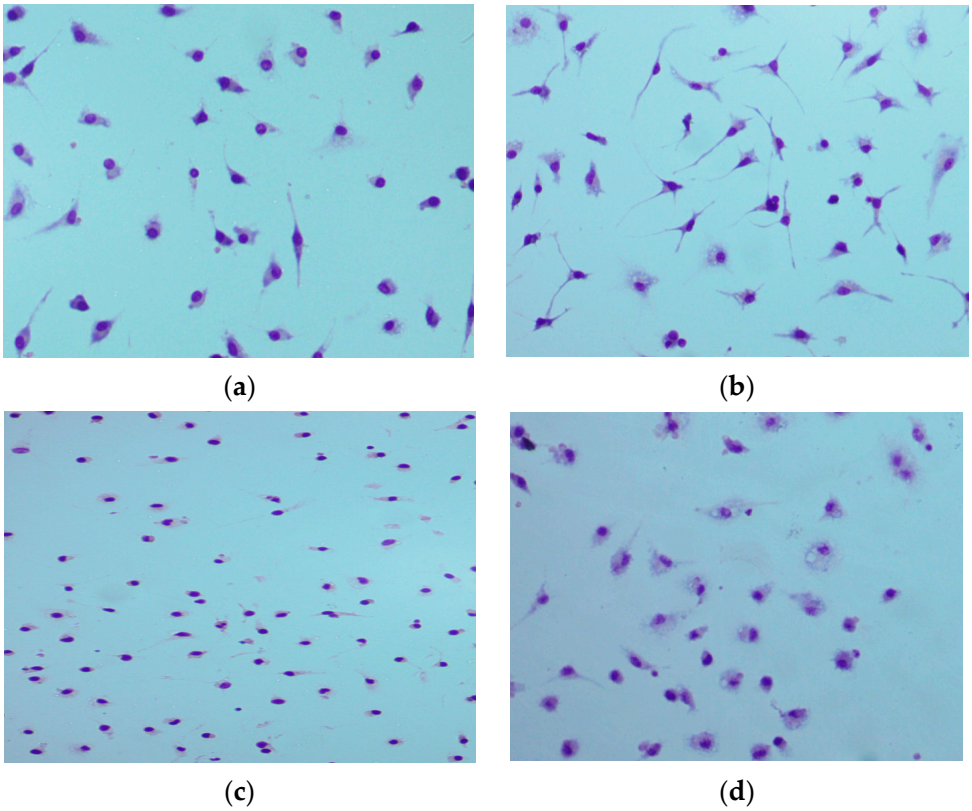

Figure 3. The effect of compound **15** and dexamethasone on the morphology of mouse peritoneal macrophages. Azur-eosin staining according to Romanovsky; magnification 200× ((**a**)—Vehicle + 2% DMSO; (**b**)—LPS + 2% DMSO; (**c**)—LPS + 10 μM **15**; (**d**)—LPS + 10 μM Dexamethasone).

3.2.5. Oxidative Burst in Neutrophils

Encouraged by the anti-inflammatory activity of **15** along with the intact morphology of macrophages, we tested the influence of compound **15** on the activation of murine neutrophils as well. There are many triterpenoids known to affect the phenotype, immune,

and oxidative responses of neutrophils, e.g., celastrol [47] and glutinone [48]. Hence, it was of interest to evaluate the influence of compound **15** on the generation of reactive oxygen species in immune cells. Phagocytosis-induced neutrophil oxidative burst is a convenient model to study this subject. Compound **15** dose-dependently suppressed the zymosan-induced formation of reactive oxygen species in mouse neutrophils with an IC_{50} of 10 μM. Reducing neutrophil oxidative response has implications for both phagocytosis efficiency and overall oxidative stress in diabetic conditions (Figure 4).

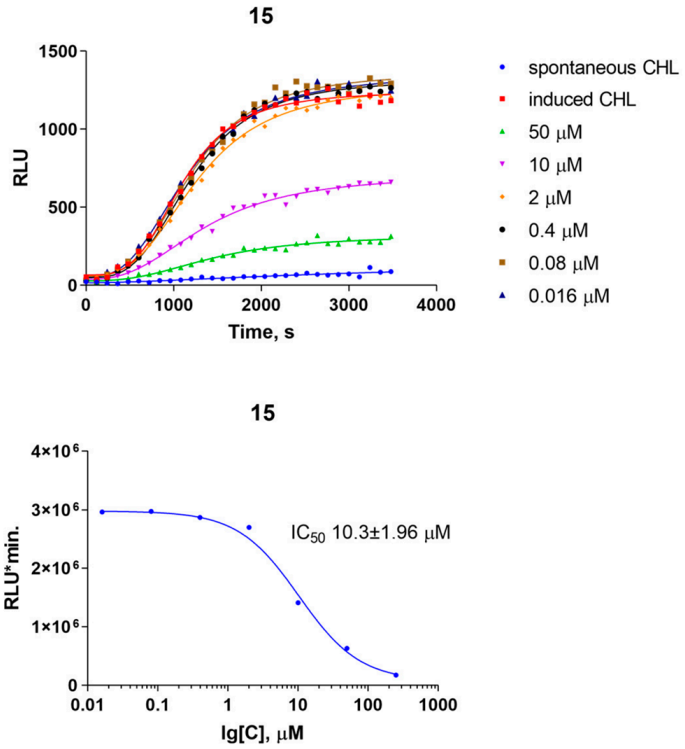

Figure 4. Compound **15** suppresses the formation of reactive oxygen species during zymosan-induced phagocytosis in mouse neutrophils. CHL—chemiluminescence.

3.2.6. Free Radical Scavenging in Cell-Free System

To discriminate ROS inhibition elicited by lead compounds in cellulo from direct free radical scavenging, we assessed the antiradical activity of lead compounds in a cell-free system. Reactive oxygen species were generated with the hemoglobin-hydrogen peroxide system and detected as luminol-mediated chemiluminescence. Compound **15** scavenges reactive oxygen species in a cell-free model system, but in concentrations an order of magnitude greater than the effective concentrations in the cellular model. Thus, the IC_{50} for direct antiradical activity is roughly 85.9 μM (see Supplementary Materials), while oxidative burst in neutrophils is inhibited two-fold at 10 μM. This indicates a specific mechanism of action (probably a protein target).

3.2.7. Glucose Uptake in Fibroblasts

To further assess the antidiabetic potential of the lead compound, a cellular model of glucose uptake was employed. Rat neonatal myocardial fibroblasts were cultivated in DMEM containing 25 mM glucose to mimic hyperglycemic conditions. Incubation of fibroblasts with 20 μM of **15** for 24 h led to a significant increase in glucose consumption but, at the same time, to a concomitant drop in viability according to the MTT test (Figure 5).

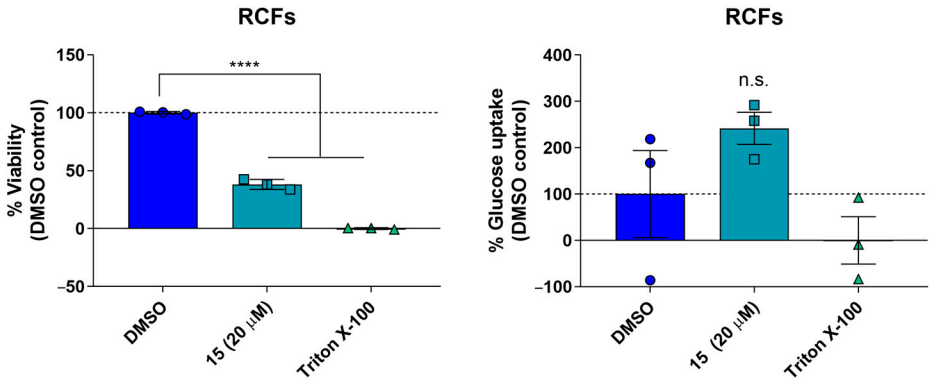

Figure 5. The compound **15** at a concentration of 20 μM after 24 h of incubation suppresses the viability of neonatal myocardial fibroblasts in rats according to the MTT test, but stimulates glucose uptake ($n = 3$). Statistical significance according to the one-way ANOVA test with the Dunnet post-test (**** $p < 0.0001$, n.s.—not significant).

3.2.8. Oral Maltose Tolerance In Vivo

Finally, the antidiabetic potential of compound **15** was evaluated in intact animals. Considering the presumed mode of action, oral maltose tolerance in rats was used. The data obtained are presented as blood glucose levels vs. time and as the areas under the glucose time curves (Figure 6). Compound **15** at a dose of 5 mg/kg prevents hyperglycemia in intact rats after a maltose load of 2 g/kg. Substance **15** at a dose of 5 mg/kg improved maltose tolerance in rats in vivo, reducing the area under the curve relative to the control by 27.3% and by 58.5% when combined with acarbose. Hence, compound **15** is orally active and improves maltose tolerance synergistically with the reference α-glucosidase inhibitor acarbose.

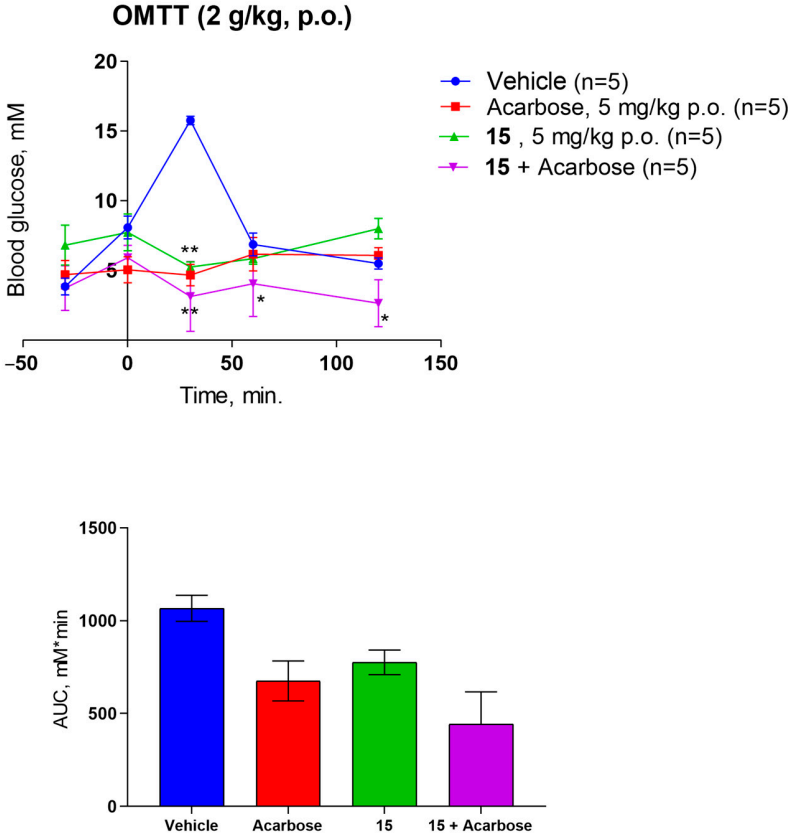

Figure 6. Antihyperglycemic activity of **15** in rats after maltose challenge. Data shown as mean ± SD. Statistical significance vs. vehicle: two-way ANOVA with Tukey post-test: * $p < 0.05$, ** $p < 0.01$.

4. Conclusions

Triterpenoids of natural and semi-synthetic origin are structurally diverse compounds enriched with biological activity. As a development of our previous works, here we report the design, synthesis, and biological evaluation of novel oleanane-type triterpenic acid derivatives against yeast α-glucosidase. We have found that the majority of compounds exhibit significant inhibitory properties. Amide derivatives of 2,3-indolo-oleanolic acid proved to be especially effective, steadily surpassing the activity of the reference drug, acarbose. *N*-methylpiperazine methylated 2,3-indolo-oleanolic propargyl amide **15** was the most active compound acting as a noncompetitive inhibitor, with K_i estimated at 3.01 μM.

We have found that compound **15** also suppresses LPS-induced NO synthesis in the low micromolar range, representing anti-inflammatory properties. Further cellular studies revealed additional diabetes-related aspects of compound **15** modes of action. It inhibits the production of reactive oxygen species during an oxidative burst in neutrophils with an IC_{50} of 10 μM. In contrast, the direct radical scavenging activity of compound **15** in a cell-free system is an order of magnitude lower, indicating that a cellular target mediates its action on neutrophils. Rat fibroblasts treated with 20 μM of **15** demonstrate a two-fold increase in glucose uptake. Hence, lead compound **15** might be able to alleviate oxidative stress, inflammation, and hyperglycemia—key pathophysiological alterations of type 2 diabetes (Figure 7).

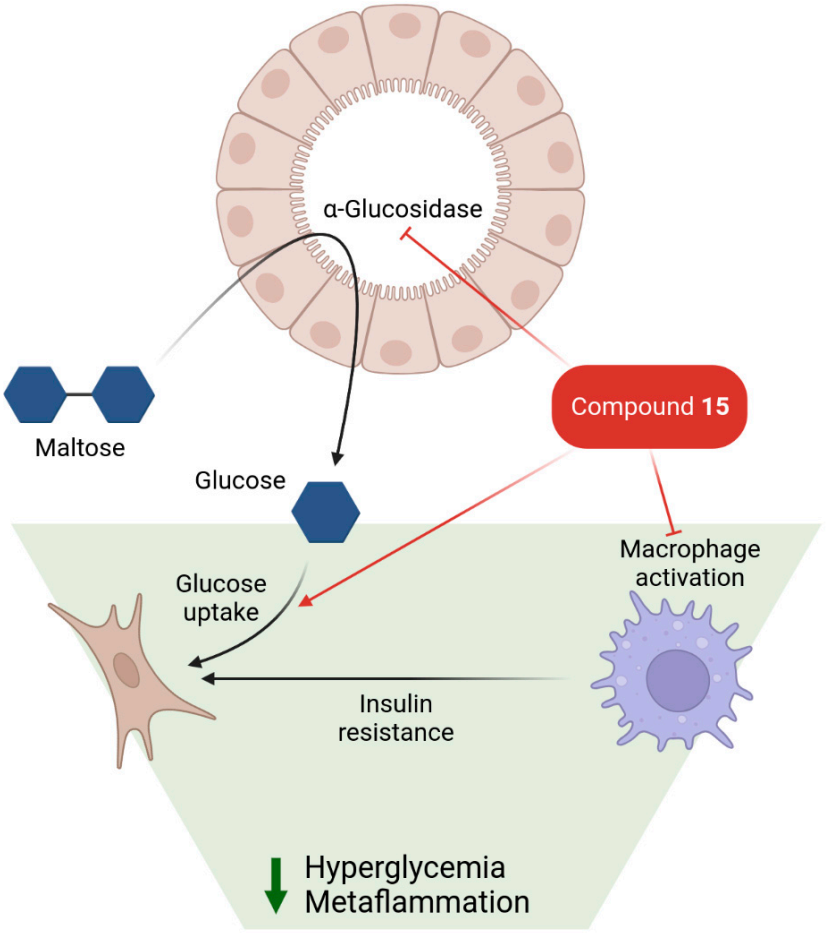

Figure 7. Proposed mechanism of antidiabetic activity of compound **15**.

The antidiabetic potential of **15** was confirmed in vivo using an oral maltose tolerance test. The treatment of rats with 5 mg/kg of **15** prevents hyperglycemia after a maltose load of 2 g/kg. Of note, we observed a synergy when the compound was co-administered with 5 mg/kg of acarbose. In conclusion, we have identified methylpiperazine methylated 2,3-

indolo-oleanolic propargyl amide **15** as a promising lead compound for the development of agents against immunometabolic disorders. Future studies are warranted to assess its safety and long-term efficacy in animal models of diabetes.

Supplementary Materials: The following supporting information can be downloaded at: https://www.mdpi.com/article/10.3390/app13169269/s1, Figure S1–S24: NMR, IR, and mass spectra of compounds **4**, **5**, **14**, **17**, **23**, and **26**, (references cited in Supplementary Materials are [49–58]).

Author Contributions: O.B.K. brought the idea, managed the chemical research and prepared the manuscript; A.V.P. and E.F.K. conducted the chemical experiments and prepared the manuscript; I.P.B. conducted the NMR experiments; D.A.B. and E.V.S. conducted the biological experiments and prepared the manuscript; A.A.S. managed the biological research. All authors have read and agreed to the published version of the manuscript.

Funding: This work was supported by Federal programs No. 1021062311392-9-1.4.1 and 1022040400061-8-1.4.1;1.4.3 (Russia).

Institutional Review Board Statement: Not applicable.

Informed Consent Statement: Not applicable.

Data Availability Statement: The data presented in this study are available on request from the corresponding authors.

Conflicts of Interest: The authors declare no conflict of interest.

References

1. Appari, M.; Channon, K.M.; McNeill, E. Metabolic Regulation of Adipose Tissue Macrophage Function in Obesity and Diabetes. *Antioxid. Redox Signal.* **2018**, *29*, 297–312. [CrossRef]
2. Kashtoh, H.; Baek, K.-H. Recent Updates on Phytoconstituent Alpha-Glucosidase Inhibitors: An Approach towards the Treatment of Type Two Diabetes. *Plants* **2022**, *11*, 2722. [CrossRef] [PubMed]
3. Coleman, R.L.; Scott, C.A.B.; Lang, Z.; Bethel, M.A.; Tuomilehto, J.; Holman, R.R. Meta-Analysis of the Impact of Alpha-Glucosidase Inhibitors on Incident Diabetes and Cardiovascular Outcomes. *Cardiovasc. Diabetol.* **2019**, *18*, 135. [CrossRef] [PubMed]
4. Khan, S.; Ullah, H.; Taha, M.; Rahim, F.; Sarfraz, M.; Iqbal, R.; Iqbal, N.; Hussain, R.; Ali Shah, S.A.; Ayub, K.; et al. Synthesis, DFT studies, molecular docking and biological activity evaluation of thiazole-sulfonamide derivatives as potent alzheimer's inhibitors. *Molecules* **2023**, *28*, 559. [CrossRef]
5. Rahim, F.; Ullah, H.; Hussain, R.; Taha, M.; Khan, S.; Nawaz, M.; Nawaz, F.; Gilani, S.J.; Jumah, M.N.B. Thiadiazole based triazole/hydrazone derivatives: Synthesis, in vitro α-glucosidase inhibitory activity and in silico molecular docking study. *J. Mol. Struct.* **2023**, *1287*, 135619. [CrossRef]
6. Hayat, S.; Ullah, H.; Rahim, F.; Ullah, I.; Taha, M.; Iqbal, N.; Khan, F.; Khan, M.S.; Shah, S.A.A.; Wadood, A.; et al. Synthesis, biological evaluation and molecular docking study of benzimidazole derivatives as α-glucosidase inhibitors and anti-diabetes candidates. *J. Mol. Struct.* **2023**, *1276*, 134774. [CrossRef]
7. Nipun, T.S.; Khatib, A.; Ibrahim, Z.; Ahmed, Q.U.; Redzwan, I.E.; Saiman, M.Z.; Supandi, F.; Primaharinastiti, R.; El-Seedi, H.R. Characterization of α-glucosidase inhibitors from *Psychotria malayana* jack leaves extract using lc-ms-based multivariate data analysis and in-silico molecular docking. *Molecules* **2020**, *25*, 5885. [CrossRef]
8. Atta-ur-Rahman; Zareen, S.; Choudhary, M.I.; Akhtar, M.N.; Khan, S.N. alpha-Glucosidase inhibitory activity of triterpenoids from *Cichorium intybus*. *J. Nat. Prod.* **2008**, *71*, 903–910. [CrossRef]
9. Ouyang, J.K.; Dong, L.M.; Xu, Q.L.; Wang, J.; Liu, S.B.; Qian, T.; Yuan, Y.F.; Tan, J.W. Triterpenoids with α-glucosidase inhibitory activity and cytotoxic activity from the leaves of Akebia trifoliata. *RSC Adv.* **2018**, *8*, 40483–40489. [CrossRef]
10. Ding, H.; Hu, X.; Xu, X.; Zhang, G.; Gong, D. Inhibitory mechanism of two allosteric inhibitors, oleanolic acid and ursolic acid on α-glucosidase. *Int. J. Biol. Macromol.* **2018**, *107 Pt B*, 1844–1855. [CrossRef]
11. Khan, A.; Khan, I.; Halim, S.A.; Rehman, N.U.; Karim, N.; Ahmad, W.; Khan, M.; Csuk, R.; Al-Harrasi, A. Anti-diabetic potential of β-boswellic acid and 11-keto-β-boswellic acid: Mechanistic insights from computational and biochemical approaches. *Biomed. Pharmacother.* **2022**, *147*, 112669. [CrossRef] [PubMed]
12. Deng, X.Y.; Ke, J.J.; Zheng, Y.Y.; Li, D.L.; Zhang, K.; Zheng, X.; Wu, J.Y.; Xiong, Z.; Wu, P.P.; Xu, X.T. Synthesis and bioactivities evaluation of oleanolic acid oxime ester derivatives as α-glucosidase and α-amylase inhibitors. *J. Enzym. Inhib. Med. Chem.* **2022**, *37*, 451–461. [CrossRef] [PubMed]
13. Tang, C.; Zhu, L.; Chen, Y.; Qin, R.; Mei, Z.; Xu, J.; Yang, G. Synthesis and biological evaluation of oleanolic acid derivative–chalcone conjugates as α-glucosidase inhibitors. *RSC Adv.* **2014**, *4*, 10862–10874. [CrossRef]

14. Ke, J.J.; Lin, J.; Zhang, X.; Wu, X.Z.; Zheng, Y.Y.; Hu, C.M.; Kang, Y.; Zhang, K.; Xiong, Z.; Ma, Z.Q. Synthesis of Benzylidene Analogs of Oleanolic Acid as Potential α-Glucosidase and α-Amylase Inhibitors. *Front. Chem.* **2022**, *10*, 911232. [CrossRef] [PubMed]
15. Wu, P.; He, H.; Ma, H.; Tu, B.; Li, J.; Guo, S.; Chen, S.; Cao, N.; Zheng, W.; Tang, X.; et al. Oleanolic acid indole derivatives as novel α-glucosidase inhibitors: Synthesis, biological evaluation, and mechanistic analysis. *Bioorg Chem.* **2021**, *107*, 104580. [CrossRef]
16. Hong, D.S.; Kurzrock, R.; Supko, J.G.; He, X.; Naing, A.; Wheler, J.; Lawrence, D.; Eder, J.P.; Meyer, C.J.; Ferguson, D.A.; et al. A phase I first-in-human trial of bardoxolone methyl in patients with advanced solid tumors and lymphomas. *Clin. Cancer Res.* **2012**, *18*, 3396–3406. [CrossRef]
17. Kazakova, O.B.; Medvedeva, N.I.; Baikova, I.P.; Tolstikov, G.A.; Lopatina, T.V.; Yunusov, M.S.; Zaprutko, L. Synthesis of triterpenoid acylates: Effective reproduction inhibitors of influenza A (H1N1) and papilloma viruses. *Russ. J. Bioorg Chem.* **2010**, *36*, 771–778. [CrossRef]
18. Reyes-Zurita, F.J.; Medina-O'Donnell, M.; Ferrer-Martin, R.M.; Rufino-Palomares, E.E.; Martin-Fonseca, S.; Rivas, F.; Martínez, A.; García-Granados, A.; Pérez-Jiménez, A.; García-Salguero, L.; et al. The oleanolic acid derivative, 3-O-succinyl-28-O-benzyl oleanolate, induces apoptosis in B16-F10 melanoma cells via the mitochondrial apoptotic pathway. *RSC Adv.* **2016**, *6*, 93590–93601. [CrossRef]
19. Spivak, A.Y.; Khalitova, R.R.; Nedopekina, D.A.; Gubaidullin, R.R. Antimicrobial properties of amine- and guanidine-functionalized derivatives of betulinic, ursolic and oleanolic acids: Synthesis and structure/activity evaluation. *Steroids* **2020**, *154*, 108530. [CrossRef]
20. Youqing, S.; Defa, S.; Jianbin, T.; Meihua, S. Oleanolic Acid Derivative as well as Preparation Method and Application Thereof. CN102532246B, 18 June 2014.
21. Khusnutdinova, E.F.; Petrova, A.V.; Kukovinets, O.S.; Kazakova, O.B. Synthesis and Cytotoxicity of 28-N-Propargylaminoalkylated 2,3-Indolotriterpenic acids. *Nat. Prod. Commun.* **2018**, *13*, 665–668. [CrossRef]
22. Kazakova, O.; Smirnova, I.; Lopatina, T.; Giniyatullina, G.; Petrova, A.; Khusnutdinova, E.; Csuk, R.; Serbian, I.; Loesche, A. Synthesis and cholinesterase inhibiting potential of A-ring azepano- and 3-amino-3,4-seco-triterpenoids. *Bioorg Chem.* **2020**, *101*, 104001. [CrossRef] [PubMed]
23. Kazakova, O.; Rubanik, L.; Smirnova, I.; Poleschuk, N.; Petrova, A.; Kapustina, Y.; Baikova, I.; Tret'yakova, E.; Khusnutdinova, E. Synthesis and in vitro activity of oleanolic acid derivatives against *Chlamydia trachomatis* and *Staphylococcus aureus*. *Med. Chem. Res.* **2021**, *30*, 1408–1418. [CrossRef]
24. Kazakova, O.; Mioc, A.; Smirnova, I.; Baikova, I.; Voicu, A.; Vlaia, L.; Macașoi, I.; Mioc, M.; Drăghici, G.; Avram, Ș.; et al. Novel Synthesized N-Ethyl-Piperazinyl-Amides of C2-Substituted Oleanonic and Ursonic Acids Exhibit Cytotoxic Effects through Apoptotic Cell Death Regulation. *Int. J. Mol. Sci.* **2021**, *22*, 10967. [CrossRef] [PubMed]
25. Khusnutdinova, E.; Petrova, A.; Zileeva, Z.; Kuzmina, U.; Zainullina, L.; Vakhitova, Y.; Babkov, D.; Kazakova, O. Novel A-Ring Chalcone Derivatives of Oleanolic and Ursolic Amides with Anti-Proliferative Effect Mediated through ROS-Triggered Apoptosis. *Int. J. Mol. Sci.* **2021**, *22*, 9796. [CrossRef]
26. Kazakova, O.B.; Brunel, J.M.; Khusnutdinova, E.F.; Negrel, S.; Giniyatullina, G.V.; Lopatina, T.V.; Petrova, A.V. A-Ring-Modified Triterpenoids and Their Spermidine–Aldimines with Strong Antibacterial Activity. *Molbank* **2019**, *2019*, M1078. [CrossRef]
27. Smirnova, I.E.; Kazakova, O.B.; Viet, D.Q.; Thuc, N.T.; Linh, T.P.; Huong, D.T.T. Synthesis and evaluation of 29-norcycloartane triterpenoids as α-glucosidase inhibitors. *Med. Chem. Res.* **2015**, *24*, 2177–2182. [CrossRef]
28. Khusnutdinova, E.F.; Smirnova, I.E.; Giniyatullina, G.V.; Medvedeva, N.I.; Yamansarov, E.Y.; Kazakov, D.V.; Kazakova, O.B.; Linh, P.T.; Viet, D.Q.; Huong, D.T. Inhibition of Alpha-Glucosidase by Synthetic Derivatives of Lupane, Oleanane, Ursane and Dammarane Triterpenoids. *Nat. Prod. Commun.* **2016**, *11*, 33–35. [CrossRef]
29. Khusnutdinova, E.F.; Smirnova, I.E.; Kazakova, O.B.; Petrova, A.V.; Ha, N.T.T.; Viet, D.Q. Synthesis and evaluation of 2,3-indolotriterpenoids as new α-glucosidase inhibitors. *Med. Chem. Res.* **2017**, *26*, 2737–2742. [CrossRef]
30. Khusnutdinova, E.F.; Petrova, A.V.; Thu, H.N.T.; Tu, A.L.T.; Thanh, T.N.; Thi, C.B.; Babkov, D.A.; Kazakova, O.B. Structural modifications of 2,3-indolobetulinic acid: Design and synthesis of highly potent α-glucosidase inhibitors. *Bioorg Chem.* **2019**, *88*, 102957. [CrossRef]
31. Wang, J.; Lu, S.; Sheng, R.; Fan, J.; Wu, W.; Guo, R. Structure-Activity Relationships of Natural and Synthetic Indole-Derived Scaffolds as α-Glucosidase Inhibitors: A Mini-Review. *Mini Rev. Med. Chem.* **2020**, *20*, 1791–1818. [CrossRef]
32. Khusnutdinova, E.F.; Ha, N.T.T.; Giniyatullina, G.V.; Anh, L.T.T.; Poptsov, A.I.; Kazakova, O.B. Synthesis and alpha—Inhibitory activity of lupane type C2-benzylidene-triterpenoids. *Vietnam. J. Chem.* **2021**, *59*, 612–619.
33. Khusnutdinova, E.; Galimova, Z.; Lobov, A.; Baikova, I.; Kazakova, O.; Thu, H.N.T.; Tuyen, N.V.; Gatilov, Y.; Csuk, R.; Serbian, I.; et al. Synthesis of messagenin and platanic acid chalcone derivatives and their biological potential. *Nat. Prod. Res.* **2022**, *36*, 5189–5198. [CrossRef] [PubMed]
34. Zhang, Y.N.; Zhang, W.; Hong, D.; Shi, L.; Shen, Q.; Li, J.Y.; Li, J.; Hu, L.H. Oleanolic acid and its derivatives: New inhibitor of protein tyrosine phosphatase 1B with cellular activities. *Bioorg. Med. Chem.* **2008**, *16*, 8697–8705. [CrossRef] [PubMed]
35. Ramírez-Espinosa, J.J.; Rios, M.Y.; Paoli, P.; Flores-Morales, V.; Camici, G.; de la Rosa-Lugo, V.; Hidalgo-Figueroa, S.; Navarrete-Vázquez, G.; Estrada-Soto, S. Synthesis of oleanolic acid derivatives: In vitro, in vivo and in silico studies for PTP-1B inhibition. *Eur. J. Med. Chem.* **2014**, *87*, 316–327. [CrossRef] [PubMed]

36. Zhang, W.; Hong, D.; Zhou, Y.; Zhang, Y.; Shen, Q.; Li, J.Y.; Hu, L.H.; Li, J. Ursolic acid and its derivative inhibit protein tyrosine phosphatase 1B, enhancing insulin receptor phosphorylation and stimulating glucose uptake. *Biochim. Et Biophys. Acta* **2006**, *1760*, 1505–1512. [CrossRef]
37. Zhao, B.T.; Nguyen, D.H.; Le, D.D.; Choi, J.S.; Min, B.S.; Woo, M.H. Protein tyrosine phosphatase 1B inhibitors from natural sources. *Arch. Pharm. Res.* **2018**, *41*, 130–161. [CrossRef]
38. Agrawal, N.K.; Kant, S. Targeting inflammation in diabetes: Newer therapeutic options. *World J. Diabetes* **2014**, *5*, 697–710. [CrossRef]
39. Liu, W.M.; Dalgleish, A.G. MTT assays can underestimate cell numbers. *Cancer Chemother. Pharmacol.* **2009**, *64*, 861–862. [CrossRef]
40. Stepanenko, A.A.; Dmitrenko, V.V. Pitfalls of the MTT assay: Direct and off-target effects of inhibitors can result in over/underestimation of cell viability. *Gene* **2015**, *574*, 193–203. [CrossRef]
41. Es-Saady, D.; Simon, A.; Jayat-Vignoles, C.; Chulia, A.J.; Delage, C. MCF-7 cell cycle arrested at G1 through ursolic acid, and increased reduction of tetrazolium salts. *Anticancer. Res.* **1996**, *16*, 481–486.
42. Gundoju, N.; Bokam, R.; Yalavarthi, N.R.; Azad, R.; Ponnapalli, M.G. Betulinic acid derivatives: A new class of α-glucosidase inhibitors and LPS-stimulated nitric oxide production inhibition on mouse macrophage RAW 264.7 cells. *Nat. Prod. Res.* **2018**, *33*, 1462182. [CrossRef] [PubMed]
43. Mosén, H.; Salehi, A.; Henningsson, R.; Lundquist, I. Nitric oxide inhibits, and carbon monoxide activates, islets acid α-glucoside hydrolase activities in parallel with glucose-stimulated insulin secretion. *J. Endocrinol.* **2006**, *190*, 681–693. [CrossRef] [PubMed]
44. Akesson, B.; Henningsson, R.; Salehi, A.; Lundquist, I. Islet constitutive nitric oxide synthase and glucose regulation of insulin release in mice. *J. Endocrinol.* **1999**, *163*, 39–48. [CrossRef] [PubMed]
45. Tian, G.; Wilcockson, D.; Perry, V.H.; Rudd, P.M.; Dwek, R.A.; Platt, F.M.; Platt, N. Inhibition of α-glucosidases I and II increases the cell surface expression of functional class A macrophage scavenger receptor (SR-A) by extending its half-life. *J. Biolog Chem.* **2004**, *279*, 39303–39309. [CrossRef] [PubMed]
46. Borenfreund, E.; Puerner, J.A. Toxicity determined in vitro by morphological alterations and neutral red absorption. *Toxicol. Lett.* **1985**, *24*, 119–124. [CrossRef] [PubMed]
47. Yu, Y.; Koehn, C.D.; Yue, Y.; Li, S.; Thiele, G.M.; Hearth-Holmes, M.P.; Mikuls, T.R.; O'Dell, J.R.; Klassen, L.W.; Zhang, Z.; et al. Celastrol Inhibits Inflammatory Stimuli-Induced Neutrophil Extracellular Trap Formation. *CMM* **2015**, *15*, 401–410. [CrossRef]
48. Sharma, K.R. Immunomodulatory Studies on Triterpenoids from Scoparia dulcis Linn. *Biochem. Pharmacol.* **2015**, *4*, 1000182. [CrossRef]
49. Elya, B.; Basah, K.; Mun'im, A.; Yuliastuti, W.; Bangun, A.; Septiana, E.K. Screening of α-Glucosidase Inhibitory Activity from Some Plants of Apocynaceae, Clusiaceae, Euphorbiaceae, and Rubiaceae. *J. Biomed. Biotechnol.* **2012**, *2012*, 281078. [CrossRef]
50. Spasov, A.A.; Babkov, D.A.; Prokhorova, T.Y.; Sturova, E.A.; Muleeva, D.R.; Demidov, M.R.; Osipov, D.V.; Osyanin, V.A.; Klimochkin, Y.N. Synthesis and biological evaluation of 2-acylbenzofuranes as novel α-glucosidase inhibitors with hypoglycemic activity. *Chem. Biol. Drug Des.* **2017**, *90*, 1184–1189. [CrossRef]
51. Fujisawa, T.; Ikegami, H.; Inoue, K.; Kawabata, Y.; Ogihara, T. Effect of two α-glucosidase inhibitors, voglibose and acarbose, on postprandial hyperglycemia correlates with subjective abdominal symptoms. *Metabolism* **2005**, *54*, 387–390. [CrossRef]
52. Lubben, T.; Clampit, J.; Stashko, M.; Trevillyan, J.; Jirousek, M.R. In Vitro Enzymatic Assays of Protein Tyrosine phosphatase 1B. In *Current Protocols in Pharmacology*; Enna, S.J., Ed.; Wiley: Hoboken, NJ, USA, 2001. [CrossRef]
53. Song, M.; Park, J.E.; Park, S.G.; Lee, D.H.; Choi, H.K.; Park, B.C.; Ryu, S.E.; Kim, J.H.; Cho, S. NSC-87877, inhibitor of SHP-1/2 PTPs, inhibits dual-specificity phosphatase 26 (DUSP26). *Biophys. Res. Commun.* **2009**, *381*, 491–495. [CrossRef] [PubMed]
54. Villarreal, F.J.; Kim, G.N.N.; Ungab, D.; Printz, M.P.; Dillmann, W.H. Identification of functional angiotensin II receptors on rat cardiac fibroblasts. *Circulation* **1993**, *88*, 2849–2861. [CrossRef] [PubMed]
55. Dubey, R.K.; Gillespie, D.G.; Mi, Z.; Jackson, E.K. Exogenous and Endogenous Adenosine Inhibits Fetal Calf Serum–Induced Growth of Rat Cardiac Fibroblasts: Role of A 2B Receptors. *Circulation* **1997**, *96*, 2656–2666. [CrossRef] [PubMed]
56. Chen, Y.; Fan, J.; Cao, L.; Han, T.; Zeng, M.; Xu, Y.; Ling, Z.; Yin, Y. Unique mechanistic insights into the beneficial effects of angiotensin-(1-7) on the prevention of cardiac fibrosis: A metabolomic analysis of primary cardiac fibroblasts. *Exp. Cell Res.* **2019**, *378*, 158–170. [CrossRef] [PubMed]
57. Kopprasch, S.; Pietzsch, J.; Graessler, J. Validation of different chemilumigenic substrates for detecting extracellular generation of reactive oxygen species by phagocytes and endothelial cells. *Luminescence* **2003**, *18*, 268–273. [CrossRef]
58. Percie du Sert, N.; Hurst, V.; Ahluwalia, A.; Alam, S.; Avey, M.T.; Baker, M.; Browne, W.J.; Clark, A.; Cuthill, I.C.; Dirnagl, U.; et al. The ARRIVE guidelines 2.0: Updated guidelines for reporting animal research. *PLOS Biol.* **2020**, *18*, e3000410. [CrossRef]